

## Supporting Information

### **Elucidating important sites and the mechanism for amyloid fibril formation by coarse-grained molecular dynamics**

Ana Rojas, Nika Maisuradze, Khatuna Kachlishvili, Harold A. Scheraga,\* Gia G. Maisuradze\*

Baker Laboratory of Chemistry and Chemical Biology, Cornell University, Ithaca, New York  
14853-1301

\*To whom correspondence may be addressed. E-mail: [has5@cornell.edu](mailto:has5@cornell.edu); [gm56@cornell.edu](mailto:gm56@cornell.edu)

**Author contributions:** G.G.M. designed the research; A.R., N.M., K.K., and G.G.M. performed the research; A.R., N.M., K.K., and G.G.M. analyzed the data; and A.R., H.A.S., and G.G.M. wrote the paper.

## Figure Captions

**Figure S1.** The UNRES model of polypeptide chains. The interaction sites are peptide-bond centers (p), and side-chain ellipsoids of different sizes (SC) attached to the corresponding  $\alpha$ -carbons with different “bond lengths”,  $b_{SC}$ . The  $\alpha$ -carbon atoms are represented by small open circles. The equilibrium distance of the  $C^\alpha \dots C^\alpha$  virtual bonds is taken as 3.8 Å, which corresponds to planar *trans* peptide groups. The geometry of the chain can be described either by the virtual-bond vectors  $\mathbf{dC}_i$  ( $C^\alpha_i \dots C^\alpha_{i+1}$ ),  $i = 1, 2, \dots, N - 1$  and  $\mathbf{dX}_i$  ( $C^\alpha_i \dots SC_i$ ),  $i = 2, 3, \dots, N - 1$  (represented by thick dashed arrows, where N is the number of residues, or in terms of virtual-bond lengths, backbone virtual-bond angles  $\theta_i$ ,  $i = 2, 3, \dots, N - 1$ , backbone virtual-bond-dihedral angles  $\gamma_i$ ,  $i = 2, 3, \dots, N - 2$ , and the angles  $\alpha_i$  and  $\beta_i$ ,  $i = 2, 3, \dots, N - 1$  that describe the location of a side chain with respect to the coordinate frame defined by  $C^{\alpha}_{i-1}$ ,  $C^{\alpha}_i$  and  $C^{\alpha}_{i+1}$ .

**Figure S2.** Free-energy landscapes (in kcal/mol) along the first three PCs for the free monomer aggregation trajectory. All panels illustrate the same FEL. Panel A shows all points in the 3-D FEL space with free energy  $< 0$  (kcal/mol), in which aggregation pathway is not clearly illustrated because of strong overlapping of points corresponding to diverse energies. Panel B illustrates the same 3D FEL with only the lowest free-energy points. The 3-D FEL illustrated in panel C is the same as 3-D FEL in panel B but from the top.

**Figure S3.** Free-energy landscapes (in kcal/mol) along the first two PCs with representative structures at the minima for three different trajectories; i.e., (A) the free monomer binds to one of the chains of the fibril template completely; (B) the free monomer binds to two different chains of the fibril template at both parallel and antiparallel orientation; (C) the

free monomer does not bind to the fibril template at all.

**Figure S4.** Free-energy profiles (FEPs),  $\mu(\theta)$  and  $\mu(\gamma)$ , along the  $\theta$  and  $\gamma$  angles (panels A and B, respectively) for three different trajectories plotted in Figure S3. Black, red and green curves correspond to FEPs computed over the trajectories plotted in panels A, B and C of Figure S3, respectively. The black numbers pertain to FEPs along the  $\theta$  and  $\gamma$  angles which include only residues of the loop; the red numbers pertain to FEPs along the  $\theta$  and  $\gamma$  angles which include only residues of  $\beta$ -strands; the green numbers pertain to FEPs along  $\theta$  and  $\gamma$  angles which include the residues from both loop and  $\beta$ -strands. The NMR-derived structural data are computed from the coordinates provided by Tycko for the structural model of an  $A\beta_{(1-40)}$  (Petkova et al<sup>13</sup>) (blue circles at the bottom of each panel).

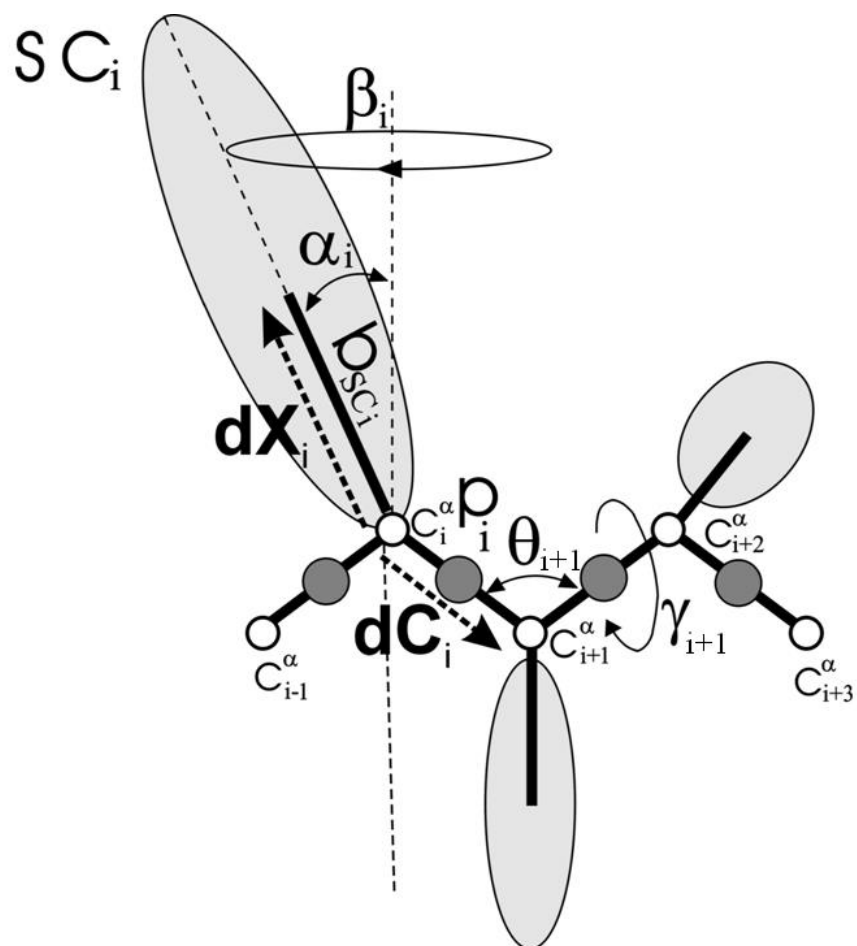


Figure S1.

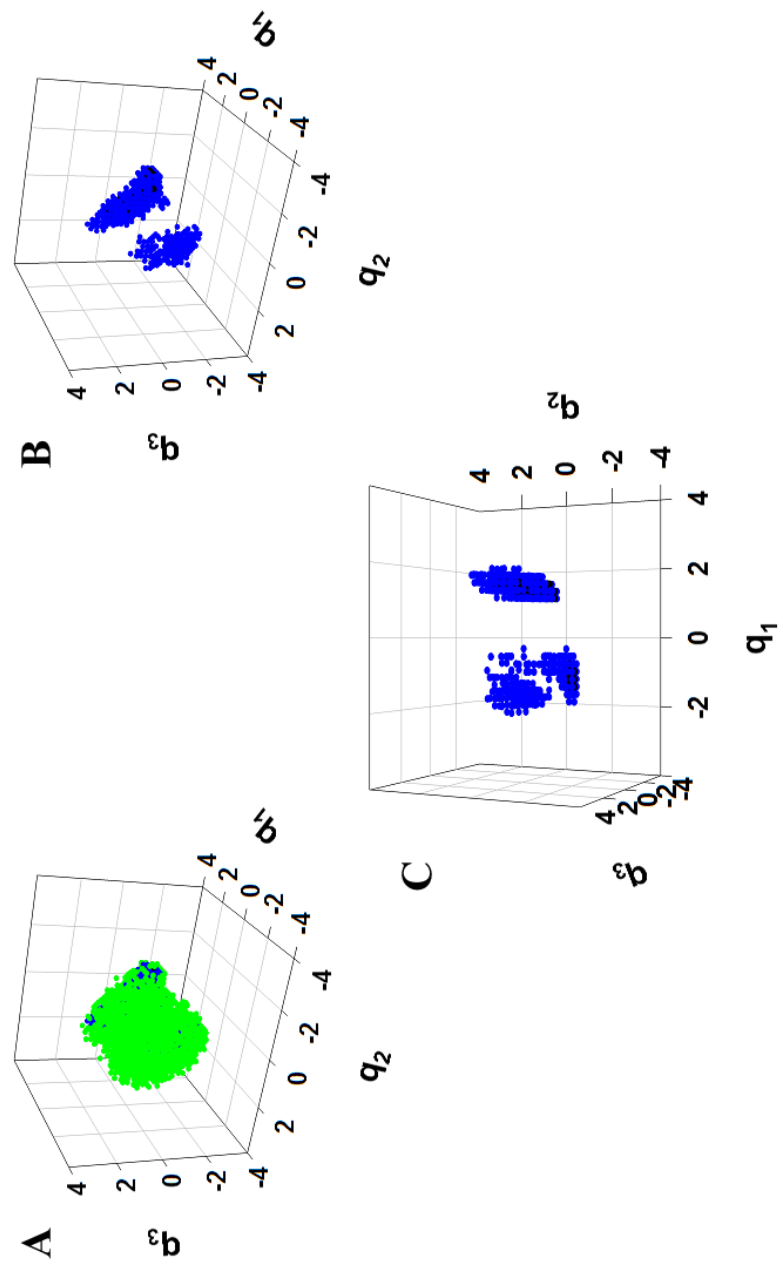


Figure S2.

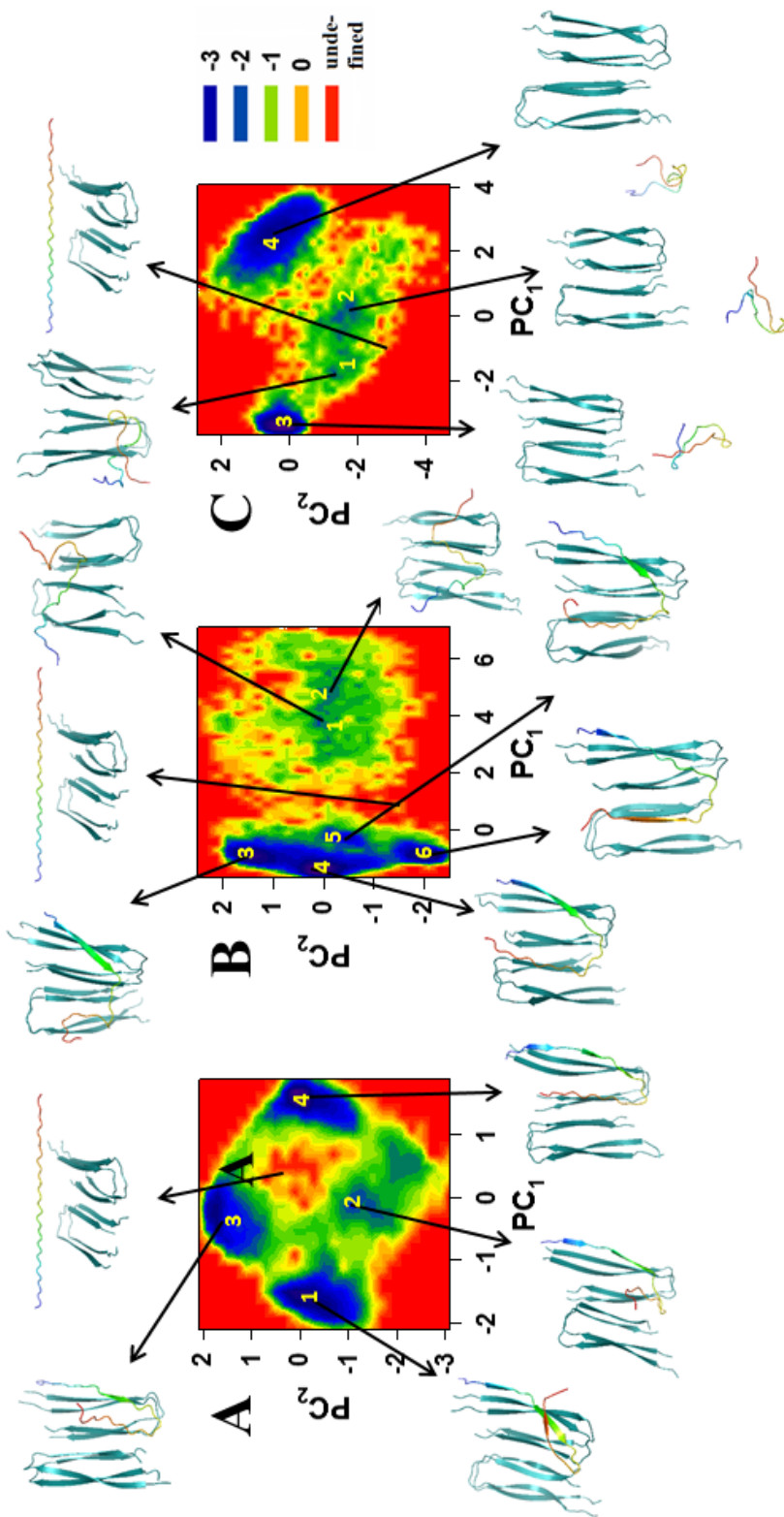


Figure S3.

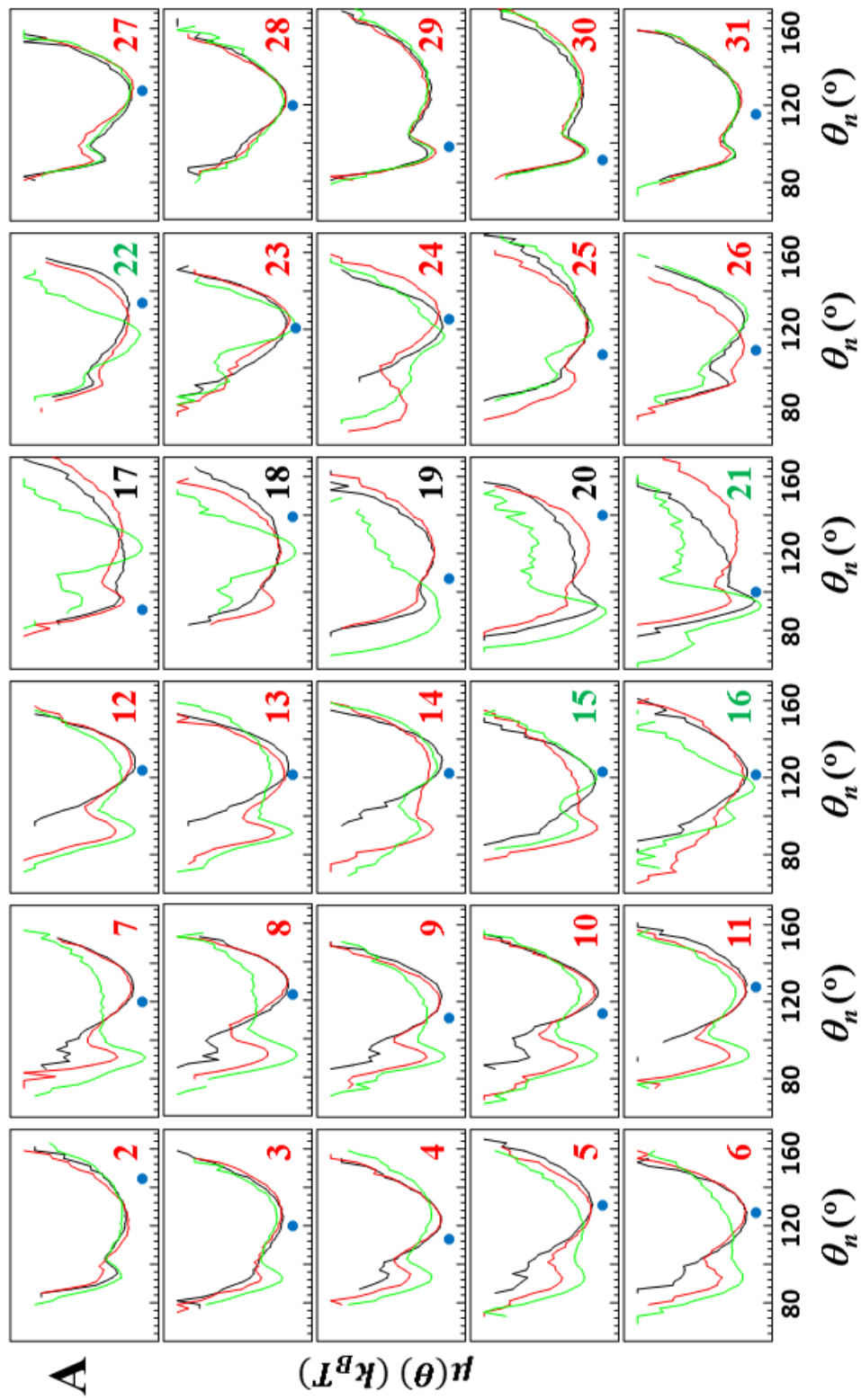


Figure S4A.

